

ISSN: 0095-8972 (Print) 1029-0389 (Online) Journal homepage: <http://www.tandfonline.com/loi/gcoo20>

Syntheses, crystal structures, and genotoxic studies of cis- μ -1,2-peroxo dicobalt(III) complexes

M. Shahid, Armeen Siddique, Istikhar A. Ansari, Farasha Sama, Sandesh Chibber, Mohd Khalid, Zafar A. Siddiqi & MD Serajul Haque Faizi

To cite this article: M. Shahid, Armeen Siddique, Istikhar A. Ansari, Farasha Sama, Sandesh Chibber, Mohd Khalid, Zafar A. Siddiqi & MD Serajul Haque Faizi (2015) Syntheses, crystal structures, and genotoxic studies of cis- μ -1,2-peroxo dicobalt(III) complexes, Journal of Coordination Chemistry, 68:5, 848-862, DOI: [10.1080/00958972.2014.1003548](https://doi.org/10.1080/00958972.2014.1003548)

To link to this article: <http://dx.doi.org/10.1080/00958972.2014.1003548>



View supplementary material [↗](#)



Accepted author version posted online: 02 Jan 2015.
Published online: 02 Feb 2015.



Submit your article to this journal [↗](#)



Article views: 62



View related articles [↗](#)



View Crossmark data [↗](#)



Citing articles: 1 View citing articles [↗](#)

Syntheses, crystal structures, and genotoxic studies of *cis*- μ -1,2-peroxo dicobalt(III) complexes

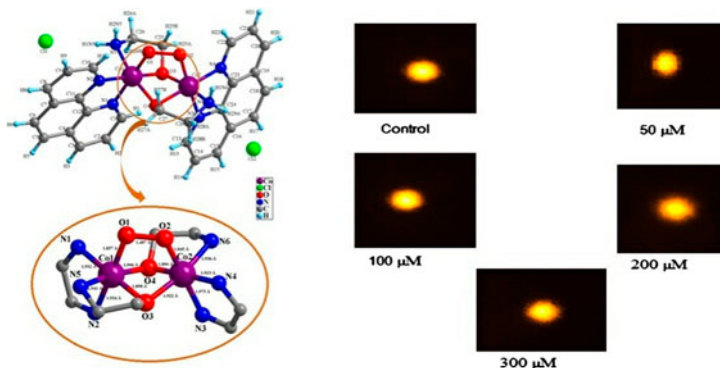
M. SHAHID†, ARMEEN SIDDIQUE†, ISTIKHAR A. ANSARI†, FARASHA SAMA†, SANDESH CHIBBER‡, MOHD KHALID†, ZAFAR A. SIDDIQI*† and MD. SERAJUL HAQUE FAIZI§

†Department of Chemistry, Aligarh Muslim University, Aligarh, India

‡Department of Biochemistry, Aligarh Muslim University, Aligarh, India

§Department of Chemistry, Indian Institute of Technology Kanpur, Kanpur, India

(Received 28 June 2014; accepted 5 December 2014)



The present work describes syntheses and X-ray studies of two unusual *cis*-peroxo bridged dinuclear Co(III) complexes. The genotoxic studies performed on the complex reveal that the complex can be exploited for industrial applications at low concentration.

Two peroxo-bridged dinuclear Co(III) complexes, $\{[\text{Co}_2(\text{ea})_2(\text{Phen})_2(\text{O}_2)] \cdot 5.5\text{H}_2\text{O} \cdot 2\text{Cl}\}$ (**1**) and $\{[\text{Co}_2(\text{ea})_2(\text{Bipy})_2(\text{O}_2)] \cdot 2\text{H}_2\text{O} \cdot 2\text{NO}_3\}$ (**2**) (Hea = ethanolamine, Phen = 1,10-phenanthroline, Bipy = 2,2'-bipyridine), are prepared by reaction of $\text{CoCl}_2 \cdot 6\text{H}_2\text{O}$ or $\text{Co}(\text{NO}_3)_2 \cdot 6\text{H}_2\text{O}$ with Hea in the presence of an α -diimine (Phen or Bipy) under reflux. The complexes have been characterized by IR, NMR, thermal gravimetric analysis, cyclic voltammetric (CV), powder X-ray diffraction, and single-crystal XRD techniques. Single-crystal X-ray crystallographic investigations of **1** and **2** reveal that each Co(III) is coordinated by one deprotonated ethanolamine and an α -diimine chelate. The remaining coordination sites of the metal ions are satisfied by bridging peroxide (O_2^{2-}) in a *cis*- μ -1,2 manner. The distances [O–O = 1.487(6) Å (**1**) and 1.462(3) Å (**2**) and $\text{Co} \cdots \text{Co} = 2.731(12)$ Å (**1**) and 2.7426(6) Å (**2**)] support the peroxo bridging in a *cis* manner in both complexes. The crystal lattice is consolidated via extensive H-bonding and π - π interactions to form a 3-D supramolecular architecture. Thermal data are consistent with the proposed stoichiometry and presence of lattice water. The CV studies of **1** indicate the presence of a quasi-reversible redox couple ($\text{Co}^{\text{III}}\text{–Co}^{\text{III}}/\text{Co}^{\text{II}}\text{–Co}^{\text{II}}$) in

*Corresponding author. Email: zafarasiddiqi@gmail.com

solution. Genotoxic studies are also performed on **1** to investigate the possible applications and side effects of the compounds in medicine.

Keywords: Peroxo-bridged dinuclear Co(III) complex; Ethanolamine; Crystal structure; Genotoxic studies

1. Introduction

Dioxygen-bridged polynuclear metal complexes have attracted attention [1, 2] of coordination and bio-inorganic chemists, owing to their potential applications in biological copper metalloproteins such as in dioxygen carrying hemocyanin in arthropods and mollusks [3–5]. Dioxygen-iron(III) complex was implicated as intermediate in the mechanisms of oxygen activating biomolecules such as cytochrome P450 and heme oxygenase [6, 7]. Peroxo-iron(III) and copper(II) species were proposed in mimicking the dioxygen activation by

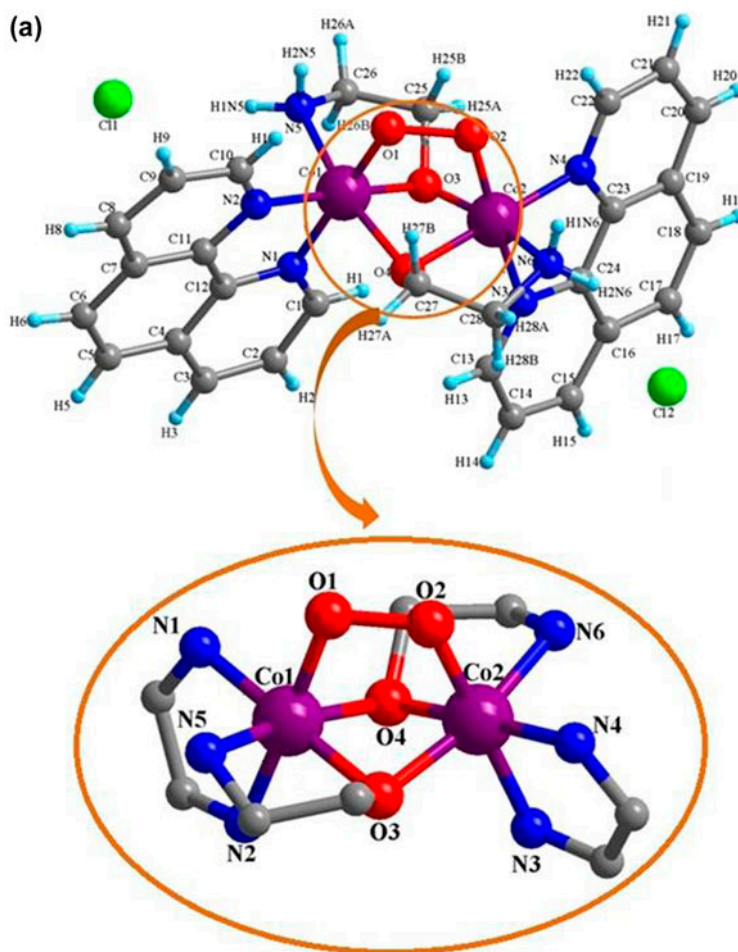


Figure 1. Molecular structures of **1** (a) and **2** (b).

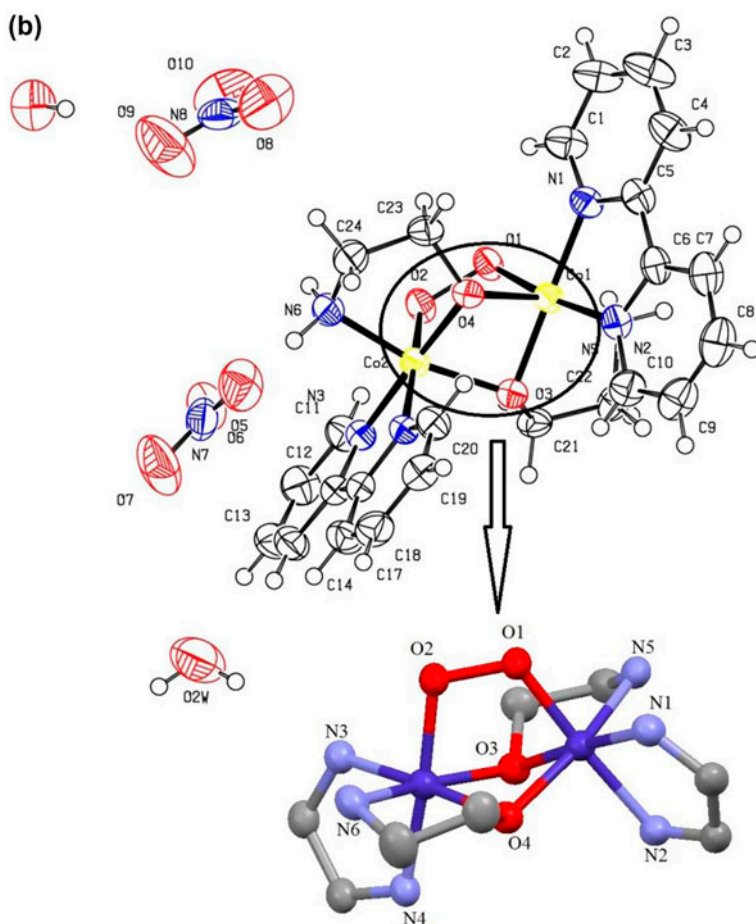
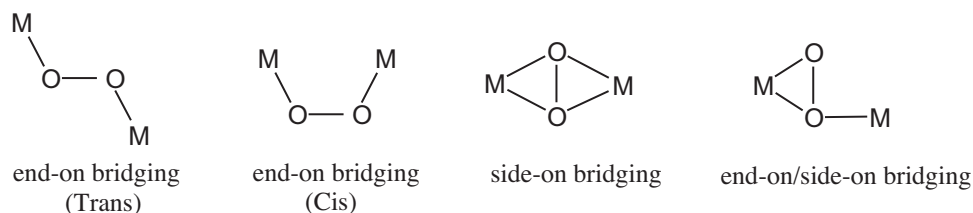


Figure 1. (Continued).

simple iron(III) [8–11] and copper(II) compounds [12–18]. A number of dioxygen-bridged coordination compounds have been reported in which the bridging dioxygen is generally a peroxide ion [19], but there are also some reports providing the binding of superoxide as bridging ligand [20–22]. Dicobalt(III) complexes involving peroxide (O_2^{2-}) [19, 23, 24] or superoxide as the only bridging unit were crystallographically characterized [25–29]. But other dioxygen-bridged dicobalt complexes also had an additional μ -amido or μ -hydroxo bridge [30–32]. In these doubly bridged dicobalt complexes, the resulting five-membered rings were almost flat.

The nature of the O–O bond in dinuclear cobalt complexes was the subject of much controversy. X-ray diffraction, vibrational, and EPR spectroscopic studies eventually allowed the distinction to be made between superoxo and peroxo ligands. There are four dioxygen (peroxo or superoxo) metal-binding coordination modes found in the bridged dinuclear compounds, *trans*- μ - $\eta^1:\eta^1$ – (end-on), μ - $\eta^2:\eta^2$ – (side-on), and μ - $\eta^1:\eta^2$ – (end-on/side-on) bridging (scheme 1) [5, 24].



Scheme 1. Various coordination modes of dioxygen species.

Table 1. Crystal data with refinement parameters for **1** and **2**.

	1	2
Empirical formula	C ₂₈ H ₃₉ Cl ₂ Co ₂ N ₆ O _{9.5}	C ₂₄ H ₃₂ Co ₂ N ₈ O ₁₂
Formula wt.	800.40	742.44
Crystal system	Triclinic	Monoclinic
Space group	<i>P</i> -1	<i>P</i> 21/ <i>c</i>
<i>a</i> (Å)	11.5852(18)	12.1158(8)
<i>b</i> (Å)	12.621(2)	18.6341(12)
<i>c</i> (Å)	13.011(2)	14.3254(10)
α (°)	64.663(3)	90
β (°)	74.819(3)	110.778(2)
γ (°)	80.711(2)	90
<i>U</i> (Å ³)	1656.8(4)	3023.9(3)
<i>Z</i>	2	4
ρ_{Calcd} (g m ⁻³)	1.406	1.631
μ (mm ⁻¹)	1.203	1.631
<i>F</i> (0 0 0)	716	1528
Refln. collected	8488	5307
Independent refln.	5725	3703
GOF	1.093	1.032
Final <i>R</i> indices [<i>I</i> > 2 σ (<i>I</i>)]	<i>R</i> ₁ = 0.0692 <i>wR</i> ₂ = 0.2252	<i>R</i> ₁ = 0.0745 <i>wR</i> ₂ = 0.1019
<i>R</i> indices (all data)	<i>R</i> ₁ = 0.0929 <i>wR</i> ₂ = 0.2457	<i>R</i> ₁ = 0.0420 <i>wR</i> ₂ = 0.0894

While the *trans*-end-on bridging mode was found in a number of Cu(II), Fe(III), and Co(III) complexes [5, 15, 23], the corresponding *cis*-end-on bridging mode was found only in complexes where the two metal centers are simultaneously doubly bridged by a peroxide and another bridging ligand such as OH⁻, O₂⁻, NH₂⁻, S₂O₃²⁻, CH₃COO⁻, PhCOO⁻, PhCH₂-COO⁻, and α -D-glucopyranosyl-(14)-D-glucose [5, 8–10, 23, 24]. μ_4 -Bridging peroxo was found in high-nuclearity cluster compounds [33–36]. Flexible amino alcohols are versatile ligands to generate di- and tetra-nuclear-bridged cobalt complexes [37]. Mixed ligand complexes of cobalt with amino alcohols (such as diethanol amine and propanol amine) and α -diimine chelator involving alkoxo or hydroxo bridging have recently been reported by our group [37]. However, dicobalt complexes of ethanolamine (Hea) with *cis*- μ -1,2 binding of bridged peroxide ion consisting of a chelator (Phen or Bipy) are not known to the best of our knowledge. Moreover, since for medicinal uses, any compound is tested first for its toxicity or side effects, genotoxic studies have also been examined for the compounds.

Table 2. Selected bond distances (Å) and angles (°) of **1** and **2**.

Complex 1			Complex 2		
Bond lengths			Bond lengths		
Co1-O1	1.857(4)	Co2-O2	1.845(4)	Co1-O1	1.841(2)
Co1-O3	1.898(5)	Co2-O3	1.922(5)	Co1-O3	1.895(2)
Co1-O4	1.906(4)	Co2-O4	1.890(5)	Co1-O4	1.914(2)
Co1-N1	1.932(6)	Co2-N3	1.975(5)	Co1-N1	1.912(3)
Co1-N2	1.934(6)	Co2-N4	1.923(6)	Co1-N2	1.950(3)
Co1-N5	1.941(7)	Co2-N6	1.936(5)	Co1-N5	1.926(3)
O1-O2	1.487(6)	Co1-Co2	2.731(12)	O1-O2	1.462(3)
Bond angles					
O1-Co1-O3	91.7(2)	O2-Co2-O4	92.89(18)	O1-Co1-O3	92.29(9)
O1-Co1-O4	87.69(19)	O4-Co2-O3	80.6(2)	O1-Co1-O4	88.43(9)
O3-Co1-O4	80.77(19)	O4-Co2-N4	91.58(19)	O3-Co1-O4	79.29(9)
O1-Co1-N2	174.2(3)	O2-Co2-N3	91.5(2)	O1-Co1-N2	173.42(11)
O3-Co1-N2	92.5(3)	O3-Co2-N3	100.7(3)	O3-Co1-N2	94.27(11)
O4-Co1-N2	89.1(2)	O2-Co2-N6	89.4(2)	O4-Co1-N2	92.24(10)
O1-Co1-N5	91.0(3)	O3-Co2-N6	167.0(2)	O1-Co1-N5	88.69(11)
O3-Co1-N5	87.2(3)	N3-Co2-N6	91.9(3)	O3-Co1-N5	87.30(10)
O4-Co1-N5	167.08(3)	O4-Co2-Col	44.21(13)	O4-Co1-N5	166.16(10)
N2-Co1-N5	93.1(3)	N4-Co2-Col	110.96(15)	N2-Co1-N5	92.17(11)
O3-Co1-N1	175.0(2)	O2-Co2-O4	92.89(18)	O3-Co1-N1	176.02(11)
O4-Co1-N1	95.0(2)	O4-Co2-O3	80.6(2)	O4-Co1-N1	98.46(10)
N2-Co1-N1	84.8(3)	O4-Co2-N4	91.58(19)	N2-Co1-N1	82.50(12)
O2-Co2-O3	87.13(19)	O2-Co2-Col	70.32(13)	O2-Co2-O3	87.81(9)
O2-Co2-N4	174.4(2)	O3-Co2-Col	44.09(15)	O2-Co2-Col	173.57(11)
O3-Co2-N4	90.2(2)	N3-Co2-Col	138.92(19)	O3-Co2-Col	92.23(10)
O4-Co2-N3	175.3(2)	O2-Co2-O3	87.13(19)	O4-Co2-N3	176.41(11)
N4-Co2-N3	84.1(2)	O2-Co2-N4	174.4(2)	N4-Co2-N3	82.52(11)
O4-Co2-N6	87.1(2)	O3-Co2-N4	90.3(2)	O4-Co2-N6	87.23(10)
N4-Co2-N6	94.2(2)	O2-Co2-Col	70.32(13)	N4-Co2-N6	91.75(11)
O2-Co2-O3	87.13(19)	O3-Co2-Col	44.02(15)	O2-Co2-Col	87.81(9)
Bond angles					
O2-Co2-O4	92.39(9)	O2-Co2-O4	92.39(9)	O2-Co2-O4	92.39(9)
O4-Co2-O3	79.25(9)	O4-Co2-O3	79.25(9)	O4-Co2-O3	79.25(9)
O4-Co2-N4	93.94(10)	O4-Co2-N4	93.94(10)	O4-Co2-N4	93.94(10)
O2-Co2-N3	91.14(11)	O2-Co2-N3	91.14(11)	O2-Co2-N3	91.14(11)
O3-Co2-N3	87.81(9)	O3-Co2-N3	87.81(9)	O3-Co2-N3	87.81(9)
O2-Co2-N6	89.71(11)	O2-Co2-N6	89.71(11)	O2-Co2-N6	89.71(11)
O3-Co2-N6	166.13(10)	O3-Co2-N6	166.13(10)	O3-Co2-N6	166.13(10)
N3-Co2-N6	93.46(11)	N3-Co2-N6	93.46(11)	N3-Co2-N6	93.46(11)
O4-Co2-Col	44.22(6)	O4-Co2-Col	44.22(6)	O4-Co2-Col	44.22(6)
N4-Co2-Col	114.81(8)	N4-Co2-Col	114.81(8)	N4-Co2-Col	114.81(8)
O2-Co2-O4	92.39(9)	O2-Co2-O4	92.39(9)	O2-Co2-O4	92.39(9)
O4-Co2-O3	79.25(9)	O4-Co2-O3	79.25(9)	O4-Co2-O3	79.25(9)
O4-Co2-N4	93.94(10)	O4-Co2-N4	93.94(10)	O4-Co2-N4	93.94(10)
O2-Co2-Col	69.33(7)	O2-Co2-Col	69.33(7)	O2-Co2-Col	69.33(7)
O3-Co2-Col	43.68(6)	O3-Co2-Col	43.68(6)	O3-Co2-Col	43.68(6)
N3-Co2-Col	137.06(8)	N3-Co2-Col	137.06(8)	N3-Co2-Col	137.06(8)
O2-Co2-O3	87.81(9)	O2-Co2-O3	87.81(9)	O2-Co2-O3	87.81(9)
O2-Co2-N4	173.57(11)	O2-Co2-N4	173.57(11)	O2-Co2-N4	173.57(11)
O3-Co2-N4	92.23(10)	O3-Co2-N4	92.23(10)	O3-Co2-N4	92.23(10)
O2-Co2-N6	69.33(7)	O2-Co2-N6	69.33(7)	O2-Co2-N6	69.33(7)
O3-Co2-Col	43.68(6)	O3-Co2-Col	43.68(6)	O3-Co2-Col	43.68(6)

2. Experimental

2.1. Synthesis of $\{[Co_2(ea)_2(Phen)_2(O_2)] \cdot 5.5H_2O \cdot 2Cl\}$ (**1**) and $\{[Co_2(ea)_2(Bipy)_2(O_2)] \cdot 2H_2O \cdot 2NO_3\}$ (**2**)

All the reaction steps were carried out in aerobic conditions. Both **1** and **2** were prepared adopting similar procedure. An aqueous solution (10 mL) of $CoCl_2 \cdot 6H_2O$ or $Co(NO_3)_2 \cdot 6H_2O$ (5 mM) was dropped to a stirred 1 : 1 mixture (clear solution) of Hea (5 mM) and Phen or Bipy (5 mM) in 20 mL methanol. The stirring was continued for 5 h at room temperature giving orange solution. The resulting solution was kept in a refrigerator giving beautiful orange-colored cubic crystals of **1** and **2** after two days. These single crystals were suitable for X-ray crystallographic studies.

Complex **1**: yield = 59%, analytical data for $C_{28}H_{43}N_6O_{11.5}Co_2Cl$, calculated (%): C = 41.94, H = 5.36, N = 10.48, Cl = 4.43; observed (%): C = 41.87, H = 5.31, N = 10.41, Cl = 4.42.

Complex **2**: yield = 54%, analytical data for $C_{24}H_{32}N_8O_{12}Co_2$, calculated (%): C = 38.83, H = 4.34, N = 15.09; observed (%): C = 38.33, H = 4.31, N = 15.22.

2.2. Materials

All reagents were of analytical grade. Ethanolamine (E. Merck), 1,10-phenanthroline (Aldrich), and 2,2'-bipyridine (Aldrich) were used as received while metal salts were recrystallized and solvents were purified by standard procedures before use [38].

2.3. Physico-chemical methods and instrumentation

IR spectra were recorded on a Perkin-Elmer spectrum GX automatic recording spectrophotometer as KBr disks. 1H and ^{13}C NMR spectra of compounds dissolved in CD_3OD were recorded on a Bruker DRC-300 spectrometer using $SiMe_4$ (TMS) as internal standard. Microanalyses for C, H, and N were obtained from Microanalytical Laboratories, CDRI, Lucknow. Thermal gravimetric analysis (TGA) data were measured from room temperature to 600 °C at a heating rate of 20 °C min^{-1} . The data were obtained using a Shimadzu TGA-50H instrument.

2.4. Crystallographic data collection and structure analysis

Single-crystal X-ray data of **1** and **2** were collected at 100 K on a Bruker SMART APEX CCD diffractometer using graphite monochromated MoK_{α} radiation ($\lambda = 0.71073 \text{ \AA}$). The linear absorption coefficients, scattering factors for the atoms, and anomalous dispersion corrections were taken from the International Tables for X-ray Crystallography [39]. The data integration and reduction were carried out with SAINT [40] software. Empirical absorption corrections were applied to the collected reflections with SADABS [41], and the space group was determined using XPREP [42]. Several DFIX commands have been given to fix the bond length parameters. The structure was solved by direct methods using SHELXTL-97 [43] and refined on F^2 by full-matrix least-squares using SHELXL-97 [44]. All non-hydrogen atoms were refined anisotropically. For **1**, squeeze refinement has been performed using PLATON that shows 5.5 water molecules per formula weight. The contribution of both the hydrogens and oxygens has been incorporated in the empirical formula

and formula weight in table 1. Pertinent crystallographic data for the compounds are summarized in tables 1 and 2.

2.5. CV studies

CV was performed on a EG&G PAR 273 potentiostat/galvanostat and an IBM PS2 computer along with EG&G M270 software to carry out the experiments and to acquire the data. The three-electrode cell configuration that comprised of a platinum sphere, a platinum plate, and Ag(s)/AgNO₃ was used as working, auxiliary, and reference electrodes, respectively. The supporting electrolyte was [nBu₄N]ClO₄. Platinum sphere electrode was sonicated for 2 min in dilute nitric acid, dilute hydrazine hydrate, and then in double-distilled water to remove the impurities. The solution was deoxygenated by bubbling research grade nitrogen, and an atmosphere of nitrogen was maintained over the solution during measurements.

2.6. Biology

2.6.1. Treatment of plasmid pUC19 DNA with compound. Reaction mixture (50 μL) contained 10 mM Tris-HCl (pH 7.5), 0.5 μg plasmid pUC19 DNA, and varied concentration of **1**. Oxidative stress by compound increased with increase in concentration. Incubation was performed at 4 °C for 2 h. After incubation, 30 μL of a solution containing 40 mM EDTA, 0.05% bromophenol blue tracking dye, and 50% (v/v) glycerol was added, and the solution was subjected to electrophoresis at 50 V in submarine 1% agarose gel. Ethidium bromide stained gel was then viewed and photographed on a UV-transilluminator.

2.6.1.1. *Isolation of lymphocytes.* Heparinized blood samples (3 mL) from a single healthy donor were obtained by venipuncture and diluted suitably in Ca²⁺- and Mg²⁺-free PBS of pH 7.5. Lymphocytes were isolated from blood using Histopaque 1077, and the cells were finally suspended in RPMI 1640 medium.

2.6.1.2. *Treatment of lymphocytes.* Lymphocytes in a total reaction volume of 2 mL were treated with varying concentration of **1**. Incubation was performed at 4 °C for 2 h; after the incubation, the reaction was processed for comet assay [45].

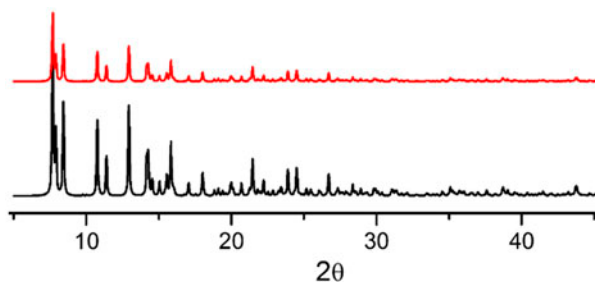


Figure 2. PXRD pattern (top – experimental, bottom – simulated) of **1**.

2.6.2. Comet assay (single cell gel electrophoresis). Comet assay was performed under alkaline conditions according to the reported procedure [46] with slight modifications. Fully frosted microscopic slides pre-coated with 1.0% normal melting agarose were used (dissolved in Ca^{+2} - and Mg^{+2} -free PBS of pH 7.5). Around 10,000 cells were mixed with 100 μL of 1.0% low melting agarose to form a cell suspension and pipetted over the first layer and covered immediately by a cover slip. The slides were placed on a flat tray and kept on ice for 10 min to solidify the agarose. The cover slips were removed, and a third layer of 0.5% low melting agarose (100 μL) was pipetted. Cover slips were placed over it, and it was allowed to solidify on ice for 5 min. The cover slips were removed, and the slides immersed in cold lysis solution containing 2.5 M NaCl, 100 mM EDTA, and 10 mM Tris, pH 10; 1% Triton X-100 was added before use for a minimum of 1.5 h at 4 $^{\circ}\text{C}$. After lysis, DNA was allowed to unwind for 20 min in alkaline electrophoretic solution consisting of 300 mM NaOH and 1 mM EDTA, pH > 13. Electrophoresis was performed at 4 $^{\circ}\text{C}$ in field strength of 0.7 V cm^{-1} and 300 mA current. The slides were then neutralized with cold 0.4 M Tris, pH 7.5, stained with 75 μL ethidium bromide (20 mg mL^{-1}), and covered with a cover slip. They were then placed in a humidified chamber to prevent drying of the gel and analyzed the same day. Slides were scored using an image analysis system (Komet 5.5; Kinetic Imaging, Liverpool, UK) attached to an Olympus (CX41) fluorescent microscope (Olympus Optical Co., Tokyo, Japan) and a COHU 4910-integrated CC camera (equipped with 510–560 nm excitation and 590 nm barrier filters) (COHU, San Diego, USA). Images from 50 cells (25 from each replicate slide) were analyzed. The parameter taken to assess lymphocytes DNA damage was tail length (migration of DNA from the nucleus in μm).

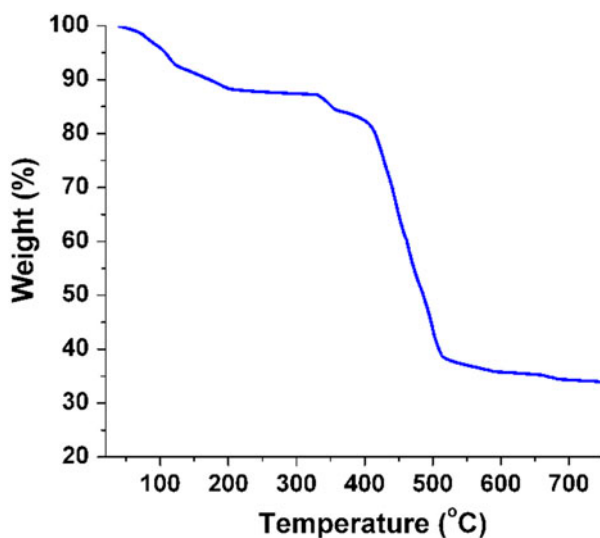


Figure 3. Thermogram of 1.

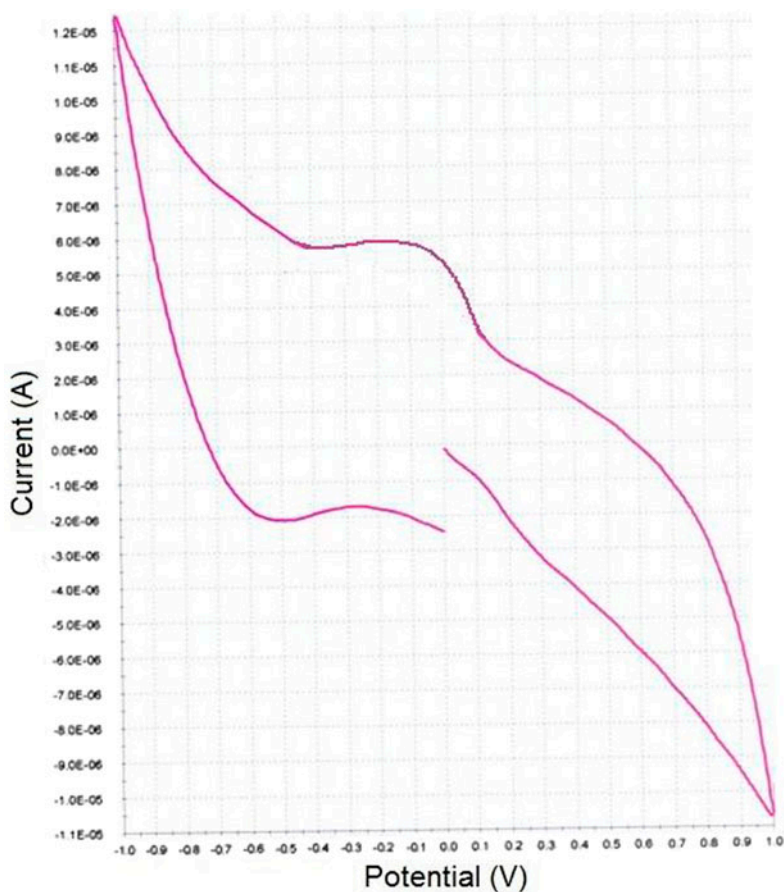


Figure 4. Scanned cyclic voltammogram of **1**.

3. Results and discussion

3.1. FTIR, ^1H and ^{13}C NMR spectra

The infrared spectra of **1** and **2** show a strong broad band at $\sim 3350\text{ cm}^{-1}$ characteristic of the presence of lattice water in the molecular unit [47]. The ligand (Hea) and its metal complexes exhibit broad bands at $3300\text{--}3350\text{ cm}^{-1}$ due to hydrogen bonded O–H bond stretch of ethanolamine. This band is, however, absent in IR spectra of the present complexes, indicating that the ligand binds the metal ions as an anionic moiety (ea^-). The band appearing at $\sim 1000\text{ cm}^{-1}$ is characteristic of bridged $\nu(\text{Co}\text{--}\text{O}\text{--}\text{Co})$ stretching vibrations in **1** and **2**. A considerable negative shift in $\nu(\text{N}\text{--}\text{H})$ frequency in the complexes relative to that of the free ligand indicates coordination from the amino nitrogen. The ligand ea^- , therefore, is a bridging ligand behaving as a bidentate [N,O] moiety. The peroxy O–O stretching frequency, $\nu(\text{O}\text{--}\text{O})$, was observed as a medium intensity band at 764 cm^{-1} (**1**) and 770 cm^{-1} (**2**), which is in the same range as that reported in structurally characterized dinuclear end-on-bridged cobalt complexes [48]. The bands observed in the low frequency $450\text{--}550\text{ cm}^{-1}$ region are

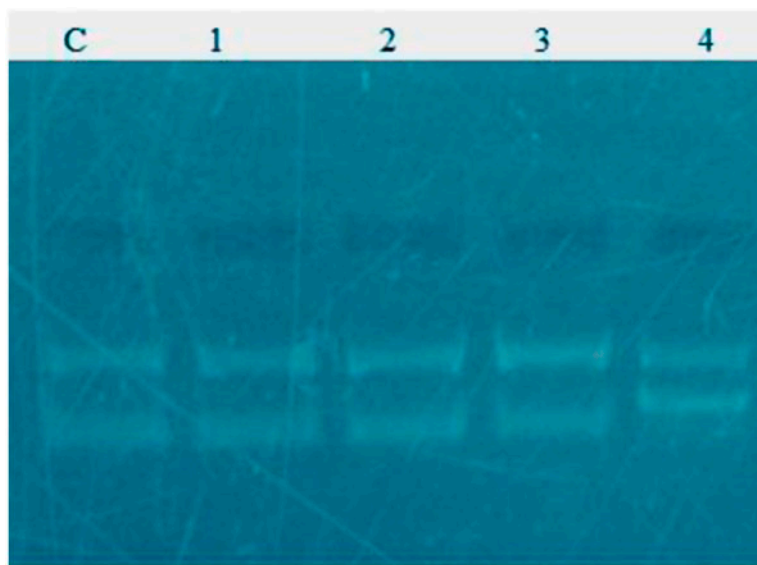


Figure 5. Effect of **1** on pUC19 DNA (plasmid nicking assay).

characteristic of M–N and M–O bond stretches [49]. The presence of the α -diimine, i.e. Phen or Bipy in the complex was ascertained from characteristic $\nu(\text{C}=\text{C})$ and $\nu(\text{C}=\text{N})$ stretching vibrations.

^1H NMR spectrum of the complexes contained a resonance on the high field side (δ 3.0–3.5 ppm) arising from the skeleton CH_2 of ea^- . The low field side (δ \sim 9.0 ppm) contained a broad signal due to N–H proton resonance. The sharp, split resonances at 7.0–8.5 ppm are characteristic of the aromatic protons of the α -diimine. There is a considerable shift in the positions of the various signals compared to that of the uncomplexed ligands, not uncommon because of the metal ion coordination [50]. The ^{13}C NMR spectra contained resonance signals at 35–43 and 125–155 ppm due to the methylene ($-\text{CH}_2-$) and α -diimine (Phen or Bipy) carbons, respectively [51, 52].

3.2. Crystal structures of $\{[\text{Co}_2(\text{ea})_2(\text{Phen})_2(\text{O}_2)] \cdot 5.5\text{H}_2\text{O} \cdot 2\text{Cl}\}$ (**1**) and $\{[\text{Co}_2(\text{ea})_2(\text{Bipy})_2(\text{O}_2)] \cdot 2\text{H}_2\text{O} \cdot 2\text{NO}_3\}$ (**2**)

Elemental analyses correlated well with the calculated values and confirmed the proposed stoichiometries of **1** and **2**. The complexes are stable in air and soluble in common organic solvents. Single-crystal X-ray diffraction reveals that **1** crystallizes in the triclinic system with $P-1$ space group and **2** crystallizes in the monoclinic system with $P21/c$ space group. The asymmetric unit of the complexes contains two crystallographically identical Co(III) metal ions, two Phen/Bipy ligands, one coordinated peroxide (bridged in *cis* manner), two coordinated ea^- , and chloride or nitrate along with water molecules in the lattice [figure 1(a) and (b)]. Crystal data with refinement parameters are given in table 1. The selected bond lengths and angles for the molecule are provided in table 2.

Each of the Co(III) ions shows a distorted octahedral CoN_3O_3 coordination from two different oxygens of each ea^- [$\text{Co}-\text{O} = 1.890(4)$ – $1.922(5)$ Å for **1** and $1.841(2)$ – $1.918(2)$ Å

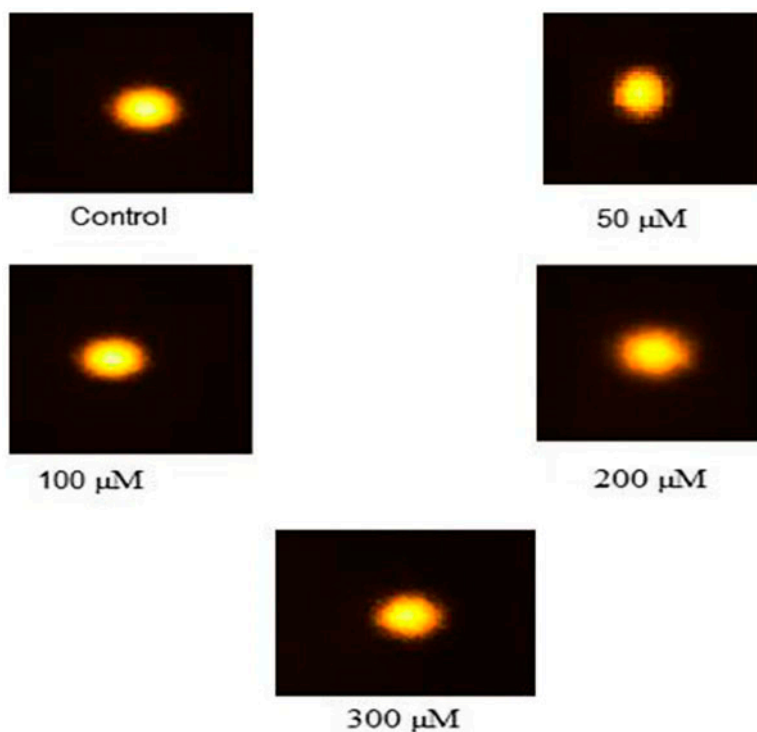


Figure 6. Single cell gel electrophoresis (comet assay) of human peripheral lymphocytes with **1**.

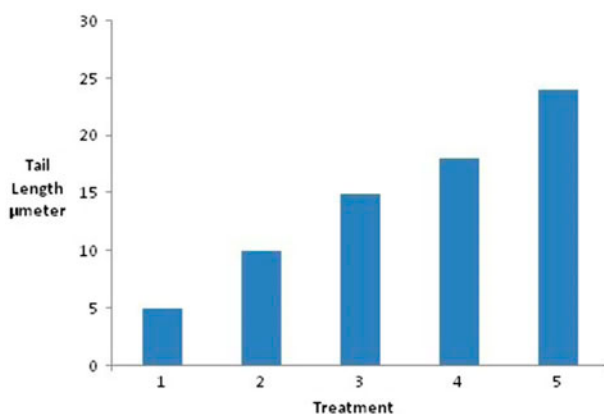


Figure 7. Effect of **1** on lymphocyte DNA breakage (% tail length).

for **2**], two nitrogens from Phen/Bipy [Co–N = 1.923(6)–1.975(5) Å for **1** and 1.912(3)–1.950(3) for **2**], and one nitrogen from ea^- [Co–N = 1.936(5), 1.941(7) Å for **1** and 1.926(3), 1.930(3) Å for **2**]. The sixth site is occupied by bridged oxygen of O_2^{2-} [O–O = 1.487(6) (**1**), 1.462(3) (**2**)].

The bridging peroxide is coordinated to both cobalt ions in a *cis*-1,2 fashion in both the complexes. All Co–O and Co–N bond distances are within the range reported for octahedral Co(III) complexes (table 2). The crystal structure shows that the molecule is stabilized by π – π aromatic stacking interactions between two neighboring Phen/Bipy ligands. The π – π aromatic stacking distances of Phen ligands are 3.28–3.53 Å. These are further reinforced by intricate non-covalent H-bonding interactions involving lattice chloride/nitrate and aromatic H to form an overall 3-D supramolecular structure [figures 1S and 2S (see online supplemental material at <http://dx.doi.org/10.1080/00958972.2014.1003548>)].

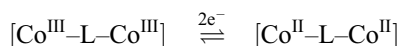
3.3. Powder X-ray diffraction and thermal (TGA) studies

The simulated and as-synthesized powder X-ray diffraction (PXRD) patterns of **1** are in excellent agreement. The pattern of as-synthesized and simulated PXRD of the compound showed no extra peaks, confirming the phase purity. The differences in intensity may be due to preferred orientations of the powdered samples as shown in figure 2.

In order to examine the thermal stability of complexes, thermal analysis of **1** was carried out in an N₂ atmosphere at the rate of 20 °C min⁻¹. The TGA of compound shows a weight loss of 12.89% (expected = 12.38%) from 80 to 210 °C that corresponds to release of all lattice water molecules [53]. Beyond this temperature (>400 °C), the compound starts to decompose (figure 3) converting into the oxide.

3.4. CV studies

The cyclic voltammogram for **1** was recorded at various scan rates (0.1, 0.2 and 0.3 V s⁻¹), and the voltammograms were similar at all scan rates due to stability of the complex in solution. The voltammogram recorded at 0.2 V s⁻¹ is given in figure 4. The voltammogram exhibited cathodic peak in the forward scan which may be coupled with the anodic peak in the reverse cycle forming a quasi-reversible redox couple with $E_{1/2}^0 = -0.17$ V. The probable electrochemical reaction involving a 2e⁻ redox mechanism may be given as follows:



The voltammogram in the present case did not indicate the existence of possible electrochemical deposition [54], unlike that reported for the homo-dinuclear complexes of Cu(II) involving macrocyclic ligands [55, 56].

3.5. Biology

In order to evaluate the possible applications of the complexes in medicines and to ascertain the side effects or effect of the complexes on DNA, genotoxic studies were performed on **1** using DNA nicking and comet assays.

3.5.1. Effect of compound on pUC19 DNA (DNA nicking assay). Nicking of plasmid DNA and its conversion to open circular form is an indication of the genotoxic nature of the compound under test. Toxic action of **1** was examined on plasmid pUC19 DNA at 50,

100, 200, and 300 μM concentrations with observation of the four forms of supercoiled DNA (figure 5). At lower concentration (50 μM), the supercoiled was neither converted to open circular nor any linear form was observed (figure 5), but at higher concentrations of the complex (100, 200, or 300 μM), the plasmid DNA is nicked and converts to open circular form with increase in the intensity of the band. This indicates that with increase in concentration of the compound, more reactive oxygen species are generated which enhance the nicking effect.

Plasmid nicking assay indicated that only negligible amount of cytotoxic damage takes place with the complex at lower concentration. Thus, **1** is non-toxic and can be exploited for medicinal applications at 50 μM concentration.

3.5.2. Effect of compound on nuclear DNA breakage (comet assay). In comet assay, the complex is treated with nuclear DNA, and the tail formation and the apparent tail length relative to the control is the index of DNA damage or in other words a measure of the toxic effect by the compound [46]. It may be noted that when **1** was added to reaction, nuclear DNA breakage (tail length) was progressively increasing with increasing concentrations of **1**. Figure 6 shows that at a concentration of 50, the tail length is least, but at higher concentrations, tail length increases remarkably. In figure 7, the data are plotted as %DNA in tail of comet, and the comparative genotoxic nature of the control and the compound (at various concentrations) can be observed. The nuclear DNA breakage (at higher concentrations of the compound) observed in our case exhibited radial movement probably due to larger fragment generation. This is presumably the result of direct interaction of compound with chromatin [57–60].

4. Conclusion

A homodinuclear Co(III) complex with *cis*-peroxide-bridging is synthesized and characterized using spectral and X-ray crystallographic techniques. The peroxo bridging is in a *cis*- μ -1,2-fashion, and the metal ions acquire distorted octahedral environments. The genotoxic studies using DNA nicking and comet assays indicate the present complex does not cause harm to human DNA at 50 μM and can be exploited for applications.

Supplementary material

The CIF files of crystal structure complexes **1** and **2** have been deposited with the CCDC Nos. 935232 and 1030840. This data can be obtained free of charge via <http://www.ccdc.cam.ac.uk/conts/retrieving.html>, or from the Cambridge Crystallographic Data Center, 12 Union Road, Cambridge CB2 1EZ, UK; Fax: +44 1223 336 033; or Email: deposit@ccdc.cam.ac.uk.

Funding

This work has been supported by the Department of Science & Technology (DST), New Delhi, India [grant number SR/FT/CS-76/2011].

References

- [1] (a) M.C. Linder, C.A. Goode. *Biochemistry of Copper*, Plenum, New York (1991); (b) W. Kaim, B. Schwederski. *Bioinorganic Chemistry: Inorganic Elements in the Chemistry of Life*, Wiley, New York (1994); (c) K.D. Karlin, Z. Tyeklar. *Bioinorganic Chemistry of Copper*, Chapman & Hall, New York (1993).
- [2] R.H. Holm, P. Kennepohl, E.I. Solomon. *Chem. Rev.*, **96**, 2239 (1996).
- [3] K.D. Karlin, A.D. Zuberbühler. In *Bioinorganic Catalysis*, R.J. Reedijk, E. Bouwman (Eds), 2nd Edn, Revised and Expanded, pp. 469–534, M. Dekker, New York (1999).
- [4] H.-C. Liang, M. Dahan, K.D. Karlin. *Curr. Opin. Chem. Biol.*, **3**, 168 (1999).
- [5] E.I. Solomon, U.M. Sundaram, T.E. Machonkin. *Chem. Rev.*, **96**, 2563 (1996).
- [6] M. Sono, M.P. Roach, E.D. Coulter, J.H. Dawson. *Chem. Rev.*, **96**, 2841 (1996).
- [7] P.R. Ortiz de Montellano. *Acc. Chem. Res.*, **31**, 543 (1998).
- [8] A.L. Feig, M. Becker, S. Schindler, R. van Eldik, S.J. Lippard. *Inorg. Chem.*, **35**, 2590 (1996).
- [9] A. Mukherjee, M.A. Cranswick, M. Chakraborti, T.K. Paine, K. Fujisawa, E. Münck, L. Que Jr. *Inorg. Chem.*, **49**, 3681 (2010).
- [10] S.V. Kryatov, F.A. Chavez, A.M. Reynolds, E.V. Rybak-Akimova, L. Que Jr., W.B. Tolman. *Inorg. Chem.*, **43**, 2141 (2004).
- [11] Y. Funahashi, T. Nishikawa, Y. Wasada-Tsutsui, Y. Kajita, S. Yamaguchi, H. Arai, T. Ozawa, K. Jitsukawa, T. Tosha, S. Hirota, T. Kitagawa, H. Masuda. *J. Am. Chem. Soc.*, **130**, 16444 (2008).
- [12] H.-C. Liang, K.D. Karlin, R. Dyson, S. Kaderli, B. Jung, A.D. Zuberbühler. *Inorg. Chem.*, **39**, 5884 (2000).
- [13] R.R. Jacobson, Z. Tyeklar, K.D. Karlin, S. Liu, J. Zubieta. *J. Am. Chem. Soc.*, **110**, 3690 (1988).
- [14] Z. Tyeklar, R.R. Jacobson, N. Wei, N.N. Murthy, J. Zubieta, K.D. Karlin. *J. Am. Chem. Soc.*, **115**, 2677 (1993).
- [15] Y. Lee, D.-H. Lee, G.Y. Park, H.R. Lucas, A.A.N. Sarjeant, M.-T. Kieber-Emmons, M.A. Vance, A.E. Milligan, E.I. Solomon, K.D. Karlin. *Inorg. Chem.*, **49**, 8873 (2010).
- [16] K.D. Karlin, S. Kaderli, A.D. Zuberbühler. *Acc. Chem. Res.*, **30**, 139 (1997).
- [17] J. Cohoy, P.L. Holland, W.B. Tolman. *Inorg. Chem.*, **38**, 2161 (1999).
- [18] T.N. Sorrell, W.K. Allen, P.S. White. *Inorg. Chem.*, **34**, 952 (1995).
- [19] K. Yamanari, M. Mori, S. Dogi, A. Fuyuhiko. *Inorg. Chem.*, **33**, 4807 (1994).
- [20] B. Spingler, M. Scanavy-Grigorieff, A. Werner, H. Berke, S.J. Lippard. *Inorg. Chem.*, **40**, 1065 (2001).
- [21] V.M. Miskowski, B.D. Santarsiero, W.P. Schaefer, G. Ansok, H.B. Gray. *Inorg. Chem.*, **23**, 172 (1984).
- [22] R. Davies, A.G. Sykes. *J. Chem. Soc. (A)*, 2237 (1968).
- [23] W.R. Harris, G.L. McLendon, A.E. Martell, R.C. Bess, M. Mason. *Inorg. Chem.*, **19**, 21 (1980).
- [24] T. Tanase, T. Onaka, M. Nakagoshi, I. Kinoshita, K. Shibata, M. Doe, J. Fujii, S. Yano. *Inorg. Chem.*, **38**, 3150 (1999).
- [25] F.R. Fronczek, W.P. Schaefer, R.E. Marsh. *Inorg. Chem.*, **14**, 611 (1975).
- [26] W.P. Schaefer, S.E. Ealick, R.E. Marsh. *Acta Crystallogr. Sec. B*, **37**, 34 (1981).
- [27] W.P. Schaefer, S.E. Ealick, D. Finley, R.E. Marsh. *Acta Crystallogr. Sec. B*, **38**, 2232 (1982).
- [28] P.V. Bernhardt, G.A. Lawrance, T.W. Hambley. *J. Chem. Soc., Dalton Trans.*, 235 (1990).
- [29] S. Schmidt, F.W. Heinemann, A. Grohmann. *Eur. J. Inorg. Chem.*, **2000**, 1657 (2000).
- [30] G.G. Christoph, R.E. Marsh, W.P. Schaefer. *Inorg. Chem.*, **8**, 291 (1969).
- [31] U. Thewalt, R.E. Marsh. *Inorg. Chem.*, **11**, 351 (1972).
- [32] U. Thewalt, G.Z. Struckmeier. *Anorg. Allg. Chem.*, **419**, 163 (1976).
- [33] I. Shweky, L.E. Pence, G.C. Papaefthymiou, R. Sessoli, J.W. Yun, A. Bino, S.J. Lippard. *J. Am. Chem. Soc.*, **119**, 1037 (1997).
- [34] F. Meyer, H. Pritzkow. *Angew. Chem. Int. Ed.*, **39**, 2112 (2000).
- [35] S. Konar, N. Bhuvanesh, A. Clearfield. *J. Am. Chem. Soc.*, **128**, 9604 (2006).
- [36] S. Khanra, S. Konar, A. Clearfield, M. Helliwell, E.J.L. McInnes, E. Tolis, F. Tuna, R.E.P. Winpenny. *Inorg. Chem.*, **48**, 5338 (2009).
- [37] Z.A. Siddiqi, A. Siddique, M. Shahid, M. Khalid, P.K. Sharma, Anjuli, M. Ahmad, S. Kumar, Y. Lan, A.K. Powell. *Dalton Trans.*, **42**, 9513 (2013).
- [38] Z.A. Siddiqi, P.K. Sharma, M. Shahid, M. Khalid, Anjuli, A. Siddique, S. Kumar. *Eur. J. Med. Chem.*, **57**, 102 (2012).
- [39] *International Tables for X-ray Crystallography*, Vol. III, Kynoch Press, Birmingham (1952).
- [40] *SAINT (Version 6.02)*, Bruker AXS, Madison, WI (1999).
- [41] G.M. Sheldrick. *SADABS: Empirical Absorption Correction Program*, University of Göttingen, Göttingen (1997).
- [42] *XPRED (Version 5.1)*, Siemens Industrial Automation Inc., Madison, WI (1995).
- [43] G.M. Sheldrick. *SHELXTL Reference Manual (Version 5.1)*, Bruker AXS, Madison, WI (1997).
- [44] G.M. Sheldrick. *SHELXL-97: Program for Crystal Structure Refinement*, University of Göttingen, Göttingen (1997).
- [45] N.P. Singh, M.T. McCoy, R.R. Tice, E.L. Schneider. *Exp. Cell. Res.*, **175**, 184 (1988).
- [46] U. Shamim, S. Hanif, M.F. Ullah, A.S. Azmi, S.H. Bhat, S.M. Hadi. *Free Radical Res.*, **42**, 764 (2008).

- [47] K. Nakamoto. *Infrared and Raman Spectra of Inorganic and Coordination Compounds*, Wiley-Interscience, New York (1986).
- [48] T.N. Sorrell, W.K. Allen, P.S. White. *Inorg. Chem.*, **34**, 952 (1995).
- [49] L.J. Bellamy. *The Infra-red Spectra of Complex Molecules*, Wiley, New York (1958).
- [50] R.S. Drago. *Physical Methods in Inorganic Chemistry*, Reinhold Pub. Corp., London (1965).
- [51] F. Lions, I.G. Dance, J. Lewis. *J. Chem. Soc. A*, 565 (1967).
- [52] B.F. Hoskins, R. Robson, G.A. Williams. *Inorg. Chim. Acta*, **16**, 121 (1976).
- [53] J.S. Kwag, M.H. Jeong, A.J. Lough, J.C. Kim. *Bull. Korean Chem. Soc.*, **31**, 2069 (2010).
- [54] Z.A. Siddiqi, V.J. Mathew. *Polyhedron*, **13**, 799 (1994).
- [55] Z.A. Siddiqi, M.M. Khan, M. Khalid, S. Kumar. *Transition Met. Chem.*, **32**, 927 (2007).
- [56] C. Dendrinou-Samara, P.D. Jannakoudakis, D.P. Kessissoglou, G.E. Manoussakis, D. Mentzafos, A. Terzis. *J. Chem. Soc., Dalton Trans.*, 3259 (1992).
- [57] S. Chibber, M. Farhan, I. Hassan, I. Naseem. *Tumor Biol.*, **33**, 701 (2012).
- [58] J.H. Lee, S.Y. Kim, I.S. Kil. *J. Biol. Chem.*, **282**, 13385 (2007).
- [59] M. Benhar, D. Engelberg, A. Levitzki. *EMBO Rep.*, **3**, 420 (2002).
- [60] C.Y. Li, S. Shan, Q. Huang, R.D. Braun, J. Lanzen, K. Hu, P. Lin, M.W. Dewhirst. *J. Natl. Cancer Inst.*, **92**, 143 (2000).